A&A 660, A91 (2022)
https://doi.org/10.1051/0004-6361/202142804

Astronomy & Astrophysics

Type III radio bursts and excitation of Langmuir waves by energetic electrons

G. Mann, C. Vocks, and A. Warmuth

Leibniz-Institut für Astrophysik Potsdam (AIP), An der Sternwarte 16, 14482 Potsdam, Germany
e-mail: gmann@aip.de

Received 1 December 2021 / Accepted 7 February 2022

ABSTRACT

Context. Solar activity occurs not only in terms of the well-known 11-year Sun spot cycle but also in terms of short-lived phenomena as radio bursts. For instance, type III radio bursts are the most common phenomenon of this activity in the Sun's radio radiation. In dynamic radio spectra, they appear as short-lived stripes of enhanced radio emission rapidly drifting from high to low frequencies. They are regarded as the radio signature of beams of energetic electrons travelling along magnetic field lines in the corona. The radio emission is thought to be plasma emission, that is to say the radio emission happens near the electron plasma frequency and/or its harmonics. Plasma emission means, that energetic electrons excite Langmuir waves, which convert into radio waves.
Aims. Initially, energetic electrons are injected in a small region in the corona. Due to their spatio-temporal evolution, they develop a beam-like velocity distribution function (VDF), which is able to excite Langmuir waves. The aim of the paper is to study the spatio-temporal behaviour of the generation of Langmuir waves under coronal cirumstances and its effect on type III radio bursts.
Methods. The generation of Langmuir waves is treated by means of the Maxwell-Vlasov equations. The results are discussed by employing plasma parameters usually found in the corona, for instance at the 150 MHz level.
Results. The Langmuir waves associated with the type III bursts are not generated by a monoenergetic electron beam, but by a population of energetic electrons with a broad velocity distribution. Hence, the Langmuir waves are produced by different parts of the energetic electron population at different times and positions.
Conclusions. In the case of type III bursts, the velocities derived from their drift rates in dynamic radio spectra are not the velocities of electrons, which generate the onset of the type III burst at a given frequency. That can lead to an apparent accelerated motion of the type III radio burst source.

Key words. Sun: radio radiation – Sun: particle emission – Sun: corona

1. Introduction

The Sun's activity occurs not only in terms of the well-known 11-year Sun spot cycle but also in terms of short-lived phenomena as flares, eruptions, coronal mass ejections (CMEs), and radio bursts (see e.g., Svestka 1981 for a review). They are also accompanied by the generation of energetic particles (see e.g., Heyvaerts 1981 for a review). Type III radio bursts are the most common phenomenon of the activity in the Sun's radio radiation (Wild 1950). They appear as short-lived stripes of enhanced radio emission rapidly drifting from high to low frequencies in the dynamic radio spectra (see e.g., Suzuki & Dulk 1985; Reid & Ratcliff 2014 for reviews). They are not necessarily flare-related. An example of type III radio bursts is presented in Fig. 1.

It was recorded by the radiospectralpolarimeter (Mann et al. 1992) of the Leibniz-Institut für Astrophysik Potsdam in Tremsdorf (Germany). At first, a type III radio burst starts at 300 MHz on 8:18:52 UT and drifts towards 110 MHz within 2 s resulting in a drift rate of $-95\,\mathrm{MHz\,s^{-1}}$. Such a value is typical for type III bursts in this frequency range (Alvarez & Haddock 1973; Aschwanden et al. 1995; Mann & Klassen 2002). Subsequently on 8:18:53 UT, a stripe of enhanced radio emission starts at 290 MHz, drifts towards lower frequencies up to a turning point at 230 MHz, and returns back towards 370 MHz. Such a burst is usually called type-U burst (Maxwell & Swarup 1958; Klein & Aurass 1993; Karlicky et al. 1996; Aurass & Klein 1997). It is interpreted as the radio signature of an electron beam propagating along a closed magnetic field line in the corona (see e.g., Suzuki & Dulk 1985).

The Sun's non-thermal radio emission is regarded as plasma emission in the MHz range (Melrose 1985). Here, energetic electrons excite Langmuir waves, which convert into escaping radio waves due to non-linear plasma processes (Melrose 1985). Hence, the emission happens near the local electron plasma frequency and/or its harmonics. The electron plasma frequency is proportional to the square root of the electron number density. Since the density is gravitationally stratified in the corona, the higher and lower frequencices are emitted in the low and high corona, respectively. If a radio source travels through the corona, it causes a frequency drift in the associated dynamic radio spectrum. Because of this relationship and the rapid drift of type III radio bursts, they are interpreted as the radio signature of beams of energetic electrons travelling along magnetic field lines through the corona (Wild 1950). If such electron beams penetrate into the interplanetary space, they can generate interplanetary type III radio bursts from the MHz down to the kHz range (see e.g., Bougeret et al. 1984). The instruments onboard the International Sun Earth Explorer (ISEE-3) spacecraft allowed for the observation of such type III bursts by in situ measurements (Lin et al. 1981). The energetic electrons associated with the type III bursts were measured in situ if they arrived at the

Article published by EDP Sciences

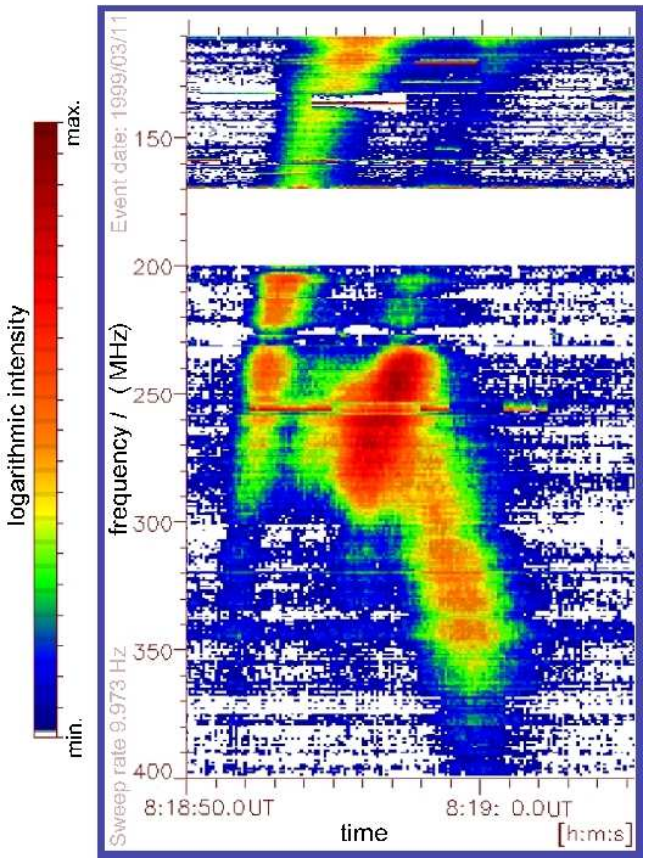

Fig. 1. Dynamic radio spectrum of a type III and type U burst in the frequency range 110–400 MHz as recorded with the radiospectralpolimeter (Mann et al. 1992) of the Leibniz-Institut fü Astrophysik Potsdam in Tremdorf (Germany). The intensity is colour coded.

spacecraft. Simultaneously, an enhanced Langmuir and radio wave level was recorded. These observations evidently support the idea, that type III bursts are generated by energetic electrons and Langmuir waves excited by them (Lin et al. 1981). This was also confirmed by measurements with the instrument onboard the WIND spacecraft (Lin et al. 1996). Thus, type III radio bursts require energetic electrons, which are able to excite Langmuir waves.

At first, Ginzburg & Zheleznyakov (1958) presented a theoretical description of type III radio bursts as a special example of a 'beam plasma interaction' in space. Then, this subject was intensely discussed by many authors (see e.g., Sturrock 1964; Zheleznyakov & Zaitsev 1970; Smith 1970; Smith et al. 1976; Melrose 1980, 1990; Goldman 1983; Dulk 1985, Kontar et al. 1998; Mel'Nik et al. 1999; Reid & Ratcliff 2014).

Radio images of solar type III radio bursts used for localizing the radio source in the corona were already made with interferometers at Culgoora (Wild 1970), Nancay (Bougeret et al. 1970), Clark Lake (Kundu et al. 1983), and the *Jansky* Very Large Array (Chen et al. 2013). Klein et al. (2008) localized the sources of type III bursts in open magnetic flux tubes by means of the Nancay radio heliograph. Mann et al. (2018) have evidently shown that the type III burst sources propagate along magnetic field lines by means of the novel interferometer 'LOw Frequency ARray' (LOFAR) (van Haarlem et al. 2013) and LOFAR's solar imaging pipeline (Breitling et al. 2015). Thus, LOFAR can operate as a dynamic spectroscopic radio imager of the Sun in the frequency range 10–90 MHz (low band – LBA) and 110–250 MHz (high band – HBA). In the special case discussed by Mann et al. (2018), the source of few type III radio bursts appearing in the LBA range propagates along closed magnetic field lines.

Magnetic reconnection is thought to be the process of energy release in the corona (see Priest 1981; Heyvaerts 1981 for reviews). Initially, a population of highly energetic electrons is produced by magnetic reconnection (see e.g., Chen et al. 2015; Shen et al. 2018; Cai et al. 2019). Since the faster electrons are overtaking the slower ones, a beam-like velocity distribution function (VDF) is developed due to the spatio-temporal evolution of this population (see e.g., Reid & Ratcliff 2014). Such a development of a beam-like VDF is studied in Sect. 2. It is well-known that a beam VDF is able to excite Langmuir waves (Baumjohann & Treumann 1997; Treumann & Baumjohann 1997). That is investigated in Sect. 3. The effect of these results on the dynamic radio spectra of type III bursts is discussed in Sect. 4. The overall results of these studies are summarized in Sect. 5.

2. Evolution of a population of energetic electrons

Magnetic reconnection is considered as the basic process of energy release in the solar corona (see e.g., Priest 1981). It can produce energetic particles (see e.g., Heyvaerts 1981 as a review) and, hence, a highly energetic electron population as well (see e.g., Chen et al. 2015). For instance, it can be observed as type III radio bursts.

Such a population of highly energetic electrons can be modelled by a reduced velocity distribution function (VDF) of the shape

$$F_{\rm v} \propto {\rm e}^{-V^2/2V_0^2}. \tag{1}$$

Here, the quantity V_0 has nothing to do with any 'thermal' velocity. It denotes the mean velocity of the highly energetic electrons. Hence, V_0 is related to the mean energy of the population of highly energetic electrons according to $\bar{E} = m_{\rm e}V_0^2/2$. Since the electrons associated with the type III radio bursts are propagating along magnetic field lines, considering only the reduced VDF is justified. The reduced VDF is obtained after the integration with respect to the velocity component perpendicular to the magnetic field.

Initially, a population with highly energetic electrons is injected at $t = 0$ and around $z = 0$ over a spatial distance of d. It can be described by a reduced VDF of the shape

$$F(V, z, t = 0) = \frac{N_{\rm h}}{\sqrt{2\pi V_0^2}} \cdot {\rm e}^{-V^2/2V_0^2} \cdot {\rm e}^{-z^2/2d^2} \tag{2}$$

We note, that this VDF is normalized to the number density $N_{\rm h}$ of the highly energetic electrons.

The spatio-temporal free evolution of a VDF F along the z-axis can be described by the well-known Liouville equation (see e.g., Baumjohann & Treumann 1997)

$$0 = \frac{\partial F}{\partial t} - V \cdot \frac{\partial F}{\partial z} \tag{3}$$

Here, the magnetic field is considered to be directed along the z-axis. (It is important to note again that the electrons associated with the type III radio bursts are travelling along the magnetic field lines). Free propagtion means no interaction, such as a wave

particle interaction and/or Coulomb collisions. Then, the spatio-temporal evolution of the VDF is found to be

$$F(V,z,t) = \frac{N_\mathrm{h}}{\sqrt{2\pi V_0^2}} \cdot \mathrm{e}^{-G(V,z,t)/2} \tag{4}$$

with

$$G(V,z,t) = \frac{V^2}{V_0^2} + \frac{(z-Vt)^2}{d^2} \tag{5}$$

After a normalization according to $W = V/V_0$, $\xi = z/d$, and $\tau = V_0 t/d$, the function G can be rewritten as

$$G = W^2 + (\xi - W\tau)^2 = (1+\tau)^2 \cdot (W - W_\mathrm{b})^2 + \frac{\xi^2}{(1+\tau^2)} \tag{6}$$

with

$$W_\mathrm{b} = \frac{\xi\tau}{(1+\tau^2)} \tag{7}$$

Finally, the reduced VDF

$$F(W,\xi,\tau) = \frac{N_\mathrm{h}}{\sqrt{2\pi V_0^2}} \cdot \exp\left(-\frac{G(W,\xi,\tau)}{2}\right) \tag{8}$$

expressed in normalized quantities represents a beam-like VDF with the beam velocity W_b and the width $(1+\tau^2)^{-1/2}$. The beam becomes narrower with running time. The beam velocity W_b has a maximum of $\max(W_\mathrm{b}) = \xi/2$ at $\tau = 1$. Asymptotically, that is $\tau \to \infty$, W_b behave like ξ/τ.

As a result, the intial VDF develops into a beam-like VDF due to its spatio-temporal evolution. It is well-known, that such a VDF is able to excite Langmuir waves (see e.g., Treumann & Baumjohann 1997). This is the subject of Sect. 3.

3. Excitation of Langmuir waves by energetic electrons

The resonant interaction of the beam electrons with the surrounding plasma leads to the excitation of Langmuir waves. The resonance condition is given by

$$0 = \omega_\mathrm{L} - V_\mathrm{res} k \tag{9}$$

(ω_L, frequency of the Langmuir wave; k, wave number of the Langmuir wave) (Baumjohann & Treumann 1997). We note that V_res is the velocity of the electrons resonantly interacting with the Langmuir waves, and ω_L is related to k by the dispersion relation

$$\omega_\mathrm{L} = \sqrt{\omega_\mathrm{pe}^2 + 3k^2 v_\mathrm{th,e}^2} \tag{10}$$

(Baumjohann & Treumann 1997). Introducing dimensionless quantities according to $\nu = \omega_L/\omega_\mathrm{pe}$ and $q = k\lambda_\mathrm{De}$ with the Debye length $\lambda_\mathrm{De} = v_\mathrm{th,e}/\omega_\mathrm{pe}$ (with ω_pe being the electron plasma frequency and $v_\mathrm{th,e}$ being the thermal electron velocity), the dispersion relation (see Eq. (10)) and the resonance condition (see Eq. (9)) can be written as

$$\nu = \sqrt{1+3q^2} \tag{11}$$

and

$$U_\mathrm{res} = \frac{\nu}{q} = \sqrt{\frac{1+3q^2}{q^2}} = \sqrt{\frac{3\nu^2}{\nu^2-1}} \tag{12}$$

with $U_\mathrm{res} = V_\mathrm{res}/v_\mathrm{th,e}$, respectively, leading to

$$q = \sqrt{\frac{1}{U_\mathrm{res}^2 - 3}} \tag{13}$$

and

$$\nu = \sqrt{\frac{U_\mathrm{res}^2}{U_\mathrm{res}^2 - 3}} \tag{14}$$

The growth and/or damping rate γ of Langmuir waves is given by Eq. (4.3) in Treumann & Baumjohann (1997). In normalized quantities, it can be expressed by

$$\frac{\gamma}{\omega_\mathrm{pe}} = \frac{\nu\pi}{2q^2 N_0} \cdot \frac{\mathrm{d}F}{\mathrm{d}U} \tag{15}$$

(with N_0 being the electron number density of the background plasma) taken at $U = U_\mathrm{res} = \nu/q$. Here, $F(U)$ is the reduced VDF. As well known, wave growth and damping occurs for $\mathrm{d}F/\mathrm{d}U > 0$ and $\mathrm{d}F/\mathrm{d}U < 0$ (see e.g., Chap. 3 in the textbook by Treumann & Baumjohann 1997), respectively. By means of Eqs. (13) and (14), one gets

$$\frac{\nu}{q^2} = U_\mathrm{res} \cdot \sqrt{U_\mathrm{res}^2 - 3} = \frac{V_0^2}{v_\mathrm{th,e}^2} \cdot W_\mathrm{res} \cdot \sqrt{W_\mathrm{res}^2 - 3 \cdot \frac{v_\mathrm{th,e}^2}{V_0^2}} \tag{16}$$

The insertion of the reduced VDF (Eq. (8)) of the energetic electrons into Eq. (15) provides

$$\frac{\gamma}{\omega_\mathrm{pe}} = \delta \cdot \sqrt{\frac{\pi}{8}} \cdot W \sqrt{W^2 - 3\frac{v_\mathrm{th,e}^2}{V_0^2}} \cdot \frac{\partial}{\partial W}\left(\exp\left[-\frac{G}{2}\right]\right) \tag{17}$$

with $\delta = N_\mathrm{h}/N_0$ taken at $W = W_\mathrm{res}$. By means of Eq. (8), one obtains for

$$\frac{\partial}{\partial W}\left(\exp\left[-\frac{G}{2}\right]\right) = (1+\tau^2) \cdot (W_\mathrm{b} - W) \cdot \exp\left[-\frac{G}{2}\right] \tag{18}$$

It shows that wave growth, that is $\gamma > 0$, occurs only for $W < W_\mathrm{b}$ The function $x \cdot \exp(-ax^2/2)$ has a local maximum at $x_\mathrm{max} = a^{-1/2}$. Hence, the growth rate (see Eq. (17)) has a maximum at

$$W_\mathrm{max} = W_\mathrm{b} - \frac{1}{(1+\tau^2)^{1/2}} \tag{19}$$

and a value of

$$\frac{\gamma_\mathrm{e,max}}{\omega_\mathrm{pe}} = \delta \cdot \sqrt{\frac{\pi}{8}} \cdot W_\mathrm{res} \sqrt{W_\mathrm{res}^2 - 3\frac{v_\mathrm{th,e}^2}{V_0^2}} \times (1+\tau^2)^{1/2} \cdot \exp\left(-\frac{1}{2}\left[1 + \frac{\xi^2}{(1+\tau^2)}\right]\right) \tag{20}$$

allowing to indentify W_res with W_max. The inspection of Eq. (19) shows that W_res approaches W_b with running time τ, i.e. $W_\mathrm{res} \to W_\mathrm{b}$ for $\tau \to \infty$. According to Eq. (20), wave growth only appears if $W_\mathrm{res} > 3^{1/2} v_\mathrm{th,e}/V_0$ is fulfilled. With Eqs. (7) and (19), this condition leads to

$$\xi > \xi_0(\tau) = \left[\frac{1}{(1+\tau^2)^{1/2}} + \frac{3^{1/2} v_{the}}{V_0}\right] \cdot \frac{(1+\tau^2)}{\tau} \tag{21}$$

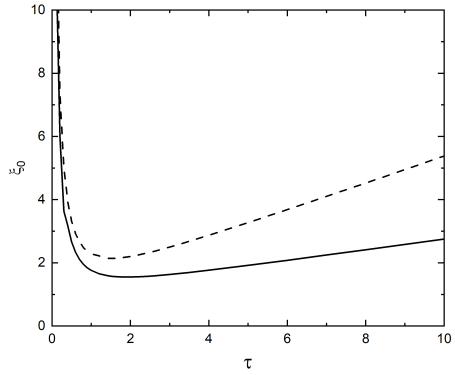

Fig. 2. Shape of the function $\xi_0(\tau)$ for $V_0 = 4v_{\rm th,e}$ (dashed line) and $V_0 = 10v_{\rm th,e}$ (solid line) according to Eq. (21). Also, $\xi > \xi_0(\tau)$ gives the area where the instability occurs in the ξ–τ-plane.

Figure 2 presents the shape of the function $\xi_0(\tau)$ for $V_0 = 4v_{\rm th,e}$ (dashed line) and $V_0 = 10v_{\rm th,e}$ (solid line) (see also the remarks in Sect. 4). Furthermore, $\xi > \xi_0(\tau)$ gives the area, where the instability occurs in the ξ–τ-plane. The function $\xi_0(\tau)$ shows local minimum at $\xi_0 = 2.140$ and $\tau = 1.5$ and at $\xi_0 = 2.550$ and $\tau = 1.9$ for $V_0 = 4v_{\rm th,e}$ and $V_0 = 10v_{\rm th,e}$, respectively. As a result, it needs a certain time and distance to develop an instability for the excitation of Langmuir waves. This subject was already discussed by Reid et al. (2014).

As previously demonstrated, the interaction of the energetic electrons with the surrounding plasma results in the excitation of Langmuir waves, on the one hand. On the other hand, the interaction of the Langmuir waves with the background plasma leads to a thermal damping as is well known (see e.g., Treumann & Baumjohann 1997). The background plasma is described by a reduced Maxwellian VDF

$$F_M(V) = \frac{N_0}{(2\pi v_{\rm th,e}^2)^{1/2}} \cdot {\rm e}^{-V^2/2v_{\rm th,e}^2} \tag{22}$$

Employing a similar approach as was done for the derivation of the increment of Langmuir wave excitation the decrement $\gamma_{\rm d}$ of the thermal damping was found to be

$$\frac{\gamma_{\rm d}}{\omega_{\rm pe}} = -\frac{V_0^3}{v_{\rm th,e}^3} \cdot \sqrt{\frac{\pi}{8}} \cdot W_{\rm res}^2 \sqrt{W_{\rm res}^2 - 3\frac{v_{\rm th,e}^2}{V_0^2}} \times \exp\left(-\frac{W_{\rm res}^2}{2}\frac{V_0^2}{v_{\rm th,e}^2}\right) \tag{23}$$

For $W_{\rm res}^2 \gg 3v_{\rm th,e}^2/V_0^2$, Eq. (22) reduces to

$$\frac{\gamma_{\rm d}}{\omega_{\rm pe}} = -\sqrt{\frac{\pi}{8}} \cdot \left(W_{\rm res}\frac{V_0}{v_{\rm th,e}}\right)^3 \cdot \exp\left(-\frac{W_{\rm res}^2}{2}\frac{V_0^2}{v_{\rm th,e}^2}\right) \tag{24}$$

The function $x^3 \cdot \exp(-x^2/2)$ has a local maximum at $x = 3^{1/2}$. Hence, thermal damping occurs strongly for $W_{\rm res} = 3^{1/2}v_{\rm th,e}/V_0$ or $V_{\rm res} = 3^{1/2}v_{\rm th,e}$ (see e.g., Treumann & Baumjohann 1997). Excitation of Langmuir waves appears only for $\gamma_{\rm e} > \gamma_{\rm d}$.

4. Discussion

In order to discuss the results of the previous section, $\delta = N_{\rm h}/N_0 = 10^{-6}$ and $V_0 = 10v_{\rm th,e}$ were chosen. We note that $V_0 = 10v_{\rm th,e}$ corresponds to a kinetic energy of 6 keV. That is typical for the mean energy of energetic electrons related to type III radio bursts (Lin et al. 1981). Here, the thermal velocity of $v_{\rm th,e} = 4604\,{\rm km\,s^{-1}}$ is adopted for a typical coronal temperature of 1.4 MK (Koutchmy 1994). The energy densities of the energetic electrons and the background ones are given by $\epsilon_{\rm h} = N_{\rm h}m_{\rm e}V_0^2/2$ and $\epsilon = 3N_0k_{\rm B}T/2$, respectively. Then, $\epsilon_{\rm h}/\epsilon_0 = \delta V_0^2/3v_{\rm th,e}^2 = 10^{-4}/3$ was found for the ratio $\epsilon_{\rm h}/\epsilon_0$. Thus, the beam electrons carry only a small fraction of the entire energy of the plasma and, hence, the beam electrons can be considered as a perturbation. That justified the approach in Sect. 3, since it is based on the linear treatment of the Maxwell–Vlasow equations (see e.g., Treumann & Baumjohann 1997).

As mentioned in Sect. 3, an instability occurs if the VDF has a region with $\mathrm{d}F/\mathrm{d}U > 0$. That causes the generation of Langmuir waves in the case under discussion. The thusly produced enhanced level of Langmuir waves acts back to the electrons due to wave particle interaction leading to the formation of a plateau in the VDF, that is $\mathrm{d}F/\mathrm{d}U = 0$. Since then, there has been no region with $\mathrm{d}F/\mathrm{d}U > 0$ in the VDF, and the instability has remained switched off. That prevents the further production of Langmuir waves. We note, that the action of the Langmuir waves back to the electrons is a non-linear process. However, studying the onset of the instability in terms of the linear Maxwell–Vlasov equations as it was done in Sect. 3 is justified and it is later discussed in this section.

Figure 1 presents a dynamic radio spectrum of a type III burst. The duration at 150 MHz is about 2.5 s. Thus, it is justified to assume, that the enhanced radio emission starts within 0.1 s. Hence, the associated Langmuir wave level should be increased at least up to 100 times the thermal one within 0.1 s. This requirement leads to $\gamma_{\rm e,max}/\omega_{\rm pe} > 4.886 \times 10^{-8}$. As a result, the growth rate must exceed this critical value for generating Langmuir and, subsequently, radio waves seen as type III radio bursts in the solar radio radiation.

Basically, the increment of wave excitation (i.e., $\gamma_{\rm e,max}$ see Eq. (20)) and the decrement of thermal damping (i.e., $\gamma_{\rm d}$ see Eq. (23)) depend on both ξ and τ. In order to study this dependence, the temporal behaviour of the quantity $(\gamma_{\rm e,max} - \gamma_{\rm d})/\omega_{\rm pe}$ must be investigated for $V_0 = 10v_{\rm th,e}$ and $\delta = 10^{-6}$, for instance. With these parameters, the damping rate $\gamma_{\rm d}/\omega_{\rm pe}$ is of the order of 10^{-19} according to Eq. (24). Hence, damping can be neglected in comparison to the wave growing at the onset of the instability. In Fig. 3, the function $\xi(\tau^*)$ is drawn for illustration purposes. The study was carried out for $\xi > 4$ in order to be sufficiently far away from the injection region $-1 < \xi < +1$ (see Eq. (2)). Here, τ^* is defined as the time τ, at which the quantity $(\gamma_{\rm e,max} - \gamma_{\rm d})/\omega_{\rm pe}$ exceeds the value 4.886×10^{-8} at a given position ξ. For instance, $(\gamma_{\rm e,max} - \gamma_{\rm d})/\omega_{\rm pe}$ exceeds the value of 4.886×10^{-8} at $\tau^* = 2.730$ and at $\xi = 10$.

The function $\xi(\tau^*)$ is not a straight line, but it is curved similar to an accelerated motion. For illustration purposes, $\Delta\xi/\Delta\tau^*$ increases from 3.509 at $\tau^* = 7$ up to 4.274 at $\tau^* = 90$, that is, it shows an apparent accelerated motion. However, that is not true. Here, the onset of the Langmuir wave generation is defined by the time τ^* at which $(\gamma_{\rm e,max} - \gamma_{\rm d})/\omega_{\rm pe}$ exceeds the value 4.886×10^{-8}. This onset is caused by electrons of different velocities $W_{\rm res}$ at different positions ξ as presented in Fig. 4. That is the reason, why the function $\xi(\tau^*)$ appears as a curved line in Fig. 3.

5. Conclusion

Solar type III radio bursts (see Fig. 1 for example) (Wild 1950) are regarded as the radio signature of beams of energetic electrons travelling along magnetic field lines through

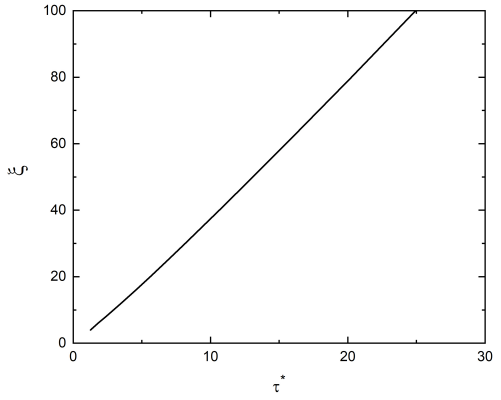

Fig. 3. Functions $\xi(\tau^*)$ for $V_0 = 10v_{\rm th,e}$ and $\delta = 10^{-6}$. The function $\xi(\tau^*)$ represents at which position ξ and time τ the increment $(\gamma_{\rm e,max} - \gamma_{\rm d})/\omega_{\rm pe}$ of the Langmuir wave excitation exceeds the value 4.886×10^{-8}.

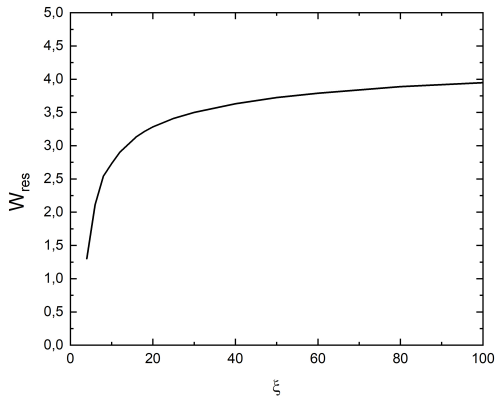

Fig. 4. Velocities $W^*_{\rm res}$ of the electrons resonantly exciting the Langmuir waves at τ^*, i.e., at the time τ_* at which the growth rate $(\gamma_{\rm e,max} - \gamma_{\rm d})/\omega_{\rm pe}$ exceeds the threshold $4.886{\times}10^{-8}$, in their dependence on the position ξ.

the corona (Wild & Smerd 1972, see also Suzuki & Dulk 1985; Reid & Ratcliff 2014 as reviews). A highly energetic electron population is produced by magnetic reconnection. It excites Langmuir waves being converted into escaping radio waves via non-linear plasma processes (Ginzburg & Zheleznyakov 1958; Melrose 1985).

Initially, a population of energetic electrons was injected in a region with the width d and was modelled by a VDF found in Eq. (1). The spatial-temporal evolution of such a population is governed by the Liouville Eq. (3). It leads to the development of a beam-like VDF with a beam velocity $W_{\rm b}$ (see Eq. (7)), which is both spatially and temporally depending. Such a VDF is able to excite Langmuir waves, which can be converted into radio waves. The growth rate (see Eq. (15)) for exciting Langmuir waves was calculated by means of the Maxwell–Vlasov equations. The thermal damping of Langmuir waves was taken into account with Eq. (23).

Figure 3 presents the spatio-temporal behaviour of the onset of the Langmuir wave generation. Initially, the Langmuir waves are excited by electrons with relative low velocities (see Fig. 4). At later times and larger distances from the injection region, they are generated by faster electons as revealed in Fig. 4. For instance, the onset of the excitation of Langmuir waves is caused by electrons with a velocity $W_{\rm res} = 3.21$ and $W_{\rm res} = 4.52$ at $\tau^* = 2.35$ and $\tau^* = 21.84$ at $\xi = 10$ and $\xi = 100$ in the case presented in Figs. 3 and 4, respectively. That leads to the apparent effect, that the onset of the Langmuir wave production, in other words the function $\xi(\tau^*)$ in Fig. 3, is caused by an agent with an accelerated motion. However, the real reason for that comes from the time of flight effects of the faster electrons and the slower ones. Furthermore, $\Delta\xi/\Delta\tau^* = 90/19.49$ provides a mean (apparent) velocity of 4.62, which is slightly higher than the velocities of the electrons that resonantly excite the Langmuir waves.

In the solar corona, the length of the acceleration (or injection) region can be assumed to be $d = 8$ Mm as deduced from other (e.g., X-ray) measurements (Masuda et al. 2000; Krucker et al. 2010; Reid et al. 2014). If a thermal electron velocity $v_{\rm th,e} = 4600\,{\rm km\,s^{-1}}$ is adopted, $\xi = 1$, $\tau = 1$, and $W = 1$ correspond to 8 Mm, 174 ms, and $46\,000\,{\rm km\,s^{-1}}$, respectively, (since $V_0 = 10v_{\rm th,e}$ was assumed in the discussion). Thus, the position ξ of the onset of the Langmuir wave excitation at τ^* travels a distance of 720 Mm within 3.39 s with a mean (apparent) velocity of $213\,000\,{\rm km\,s^{-1}}$.

In reality, the energetic electrons associated with type III radio bursts are propagating in a medium with a density inhomogeneity. That causes the rapid drift of these bursts in dynamic radio spectra. Nevertheless, the results of this paper reveal, that a type III radio burst is not generated by a monoenergetic electron beam, but by a population of energetic electrons with a broad velocity distribution (see Eq. (1)), that is to say different parts of the energetic electron population are responsible for the Langmuir wave excitation at different positions and different times as well as for the radio emission at different frequencies at different times. That can lead to an apparent accelerated motion of the type III burst source. Such an effect was really observed with LOFAR by Mann et al. (2018). This result leads to the conclusion, that the velocity derived from the drift rate (see e.g., Fig. 1) is not exactly the velocity of the electrons, which cause the onset of a type III radio burst at a fixed frequency.

References

Alvarez, H., & Haddock, F. T. 1973, Solar Phys., 29, 197
Aschwanden, M. J., Benz, A. O., Dennis, B. R., & Schwartz, R. A. 1995, ApJ, 455, 347
Aurass, H., & Klein, K.-L. 1997, A&AS, 123, 279
Baumjohann, W., & Treumann, R. A. 1997, Basic Space Plasma Physics (London: Imperial College Press), 202
Bougeret, J.-L., Caroubalos, C., Mercier, C., & Pick, M. 1970, A&A, 6, 406
Bougeret, J. L., King, J. H., & Schwenn, R. 1984, Sol. Phys., 90, 401
Breitling, F., Mann, G., Vocks, C., Steinmetz, M., & Strassmeier, K. G. 2015, Astron. Comput., 13, 99
Cai, Q., Shen, C., Raymond, J. C., et al. 2019, MNRAS, 489, 3183
Chen, B., Bastian, T. S., White, S. M., et al. 2013, ApJ, 763, L21
Chen, B., Bastian, T. S., Shen, C., et al. 2015, Science, 350, 1238
Dulk, G. A. 1985, ARA&A, 23, 189
Ginzburg, V. L., & Zheleznyakov, V. V. 1958, Sov. Astron., 2, 653
Goldman, M. V. 1983, Sol. Phys., 89, 403
Heyvaerts, J. 1981, Solar Magnetohydrodynamics (New York: Gordon and Breach Sci. Publ.), ed. E. R. Priest, 119
Karlicky, M., Mann, G., & Aurass, H. 1996, A&A, 314, 303
Klein, K.-L., & Aurass, H. 1993, AdSpR, 13, 2952008
Klein, K.-L., Krucker, S., Lantier, G., & Kerdraon, A. 2008, A&A, 486, 589
Kontar, E. P., Lapshin, V. I., & Mel'Nik, V. N. 1998, Plasma Phys. Rep., 24, 772
Koutchmy, S. 1994, AdSpR, 14, 29
Krucker, S., Hudson, H. S., Glesener, L., et al. 2010, ApJ, 714, 1108
Kundu, M. R., Gergeley, T. E., Turner, P. J., & Howard, R. A. 1983, ApJ, 269, L67
Lin, R. P., Potter, D. W., Gurnett, D. A., & Scarf, F. L. 1981, ApJ, 251, 3642
Lin, R. P., Larson, D., McFadden, J., et al. 1996, Geophys. Res. Lett., 23, 1211
Mann, G., & Klassen, A. 2002, ESA-SP, 506, 245
Mann, G., Aurass, H., Voigt, W., & Paschke, J. 1992, ESA-SP, 348, 129
Mann, G., Breitling, F., Vocks, C., et al. 2018, A&A, 611, A57
Masuda, S., Sato, J., & Kosugi, T. 2000, AdSpR, 26, 483
Maxwell, A., & Swarup, G. 1958, Nature, 181, 36
Mel'Nik, V. N., Lapshin, V., & Kontar, E. P. 1999, Sol. Phys., 184, 353
Melrose, D. B. 1980, Space Sci. Rev., 26, 3

Melrose, D. 1985, Solar Radio Physics (Cambridge: Cambridge Univ. Press), eds. D. J. McLean, & N. R. Labrum, 177
Melrose, D. B. 1990, Solar Phys., 111, 89
Priest, E. R. 1981, Solar Magnetohydrodynamics (New York: Gordon and Breach Sci. Publ.), 1999
Reid, H. A. S., & Ratcliff, H. 2014, Res. Astron. Astrophys., 14, 773
Reid, H. A. S., Vilmer, N., & Kontar, E. P. 2014, A&A, 567, A85
Shen, C., Kong, X., Guo, F., Raymond, J. C., & Chen, B. 2018, ApJ, 869, 116
Smith, D. F. 1970, Sol. Phys., 15, 202
Smith, D. F., Goldstein, M. L., & Papadopoulos, K. 1976, Sol. Phys., 46, 515
Sturrock, P. A. 1964, NASA Special Publ., 50, 357
Suzuki, S., & Dulk, G. A. 1985, Solar Radio Physics (Cambridge: Cambridge Univ. Press), eds. D. J. McLean, & N. R. Labrum, 289
Svestka, Z. 1981, Solar Magnetohydrodynamics (New York: Gordon and Breach Sci. Publ.), ed. E. R. Priest, 33
Treumann, R. A., & Baumjohann, W. 1997, Advance Space Plasma Physics (London: Imperial College Press), 69
van Haarlem, M. P., Wise, M. W., Gunst, A. W., et al. 2013, A&A, 556, A2
Wild, J. P. 1950, Aust. J. Sci. Res. Ser. A, 3, 541
Wild, J. P. 1970, PASA, 1, 365
Wild, J. P., & Smerd, S. F. 1972, ARA&A, 10, 159
Zheleznyakov, V. V., & Zaitsev, V. V. 1970, Sov. Astron., 14, 47